Stored Electromagnetic Energy and Antenna Q

Mats Gustafsson*and B. L. G. Jonsson†

November 23, 2012

Abstract

Decomposition of the electromagnetic energy into its stored and radiated parts is instrumental in the evaluation of antenna Q and the corresponding fundamental limitations on antennas. This decomposition is not unique and there several proposals in the literature. Here, it is shown that stored energy defined from the difference between the energy density and the far field energy equals the new energy expressions proposed by Vandenbosch for many cases. This also explains the observed cases with negative stored energy and suggests a possible remedy to them. The results are compared with the classical explicit expressions for spherical regions. It is shown that the results only differ by a factor ka that is interpreted as the far-field energy in the interior of the sphere. Numerical results of the Q-factors for dipole, loop, and inverted L-antennas are also compared with estimates from circuit models and differentiation of the impedance.

1 Introduction

It is well known that the electrostatic energy in free space can be written as an integral of the energy density, $\epsilon_0|\boldsymbol{E}|^2/4$, or equivalently as an integral of the electric potential, ϕ, times the charge density, ρ, [1–4]. A similar expression holds for the magnetostatic energy. The electrodynamic case is more involved. In [5], Carpenter suggests a generalization in the time domain based on $\phi\rho + \boldsymbol{A}\cdot\boldsymbol{J}$, *i.e.*, the sum of the scalar potential times the charge density and the vector potential, $\boldsymbol{A}$, times the electric current density, $\boldsymbol{J}$, see also [6, 7]. In [8], Vandenbosch presents general integral expressions in the electric current density for the stored electric and magnetic energies. These expressions are similar to the expressions by Carpenter but include some correction terms, see also [9].

*Department of Electrical and Information Technology, Lund University, Box 118, SE-221 00 Lund, Sweden. (Email: mats.gustafsson@eit.lth.se).

†Electromagnetic Engineering Lab, School of Electrical Engineering, Royal Institute of Technology, Teknikringen 33, SE-100 44 Stockholm, Sweden. (Email: lars.jonsson@ee.kth.se)

The expressions by Vandenbosch are very useful to analyze small antennas [10–13] and have been verified for wire antennas in [14]. One minor problem with the proposed expressions is that they can produce negative values of stored energy for electrically large structures [11]. On the other hand, the classical work by Chu [15] is based on subtraction of the power flow and explicit calculations using mode expansions of the stored energy outside a sphere, see also [16]. This gives simple expressions for the minimum Q of small spherical antennas [15, 16]. The major shortcoming is that the results are restricted to spherical regions although some generalizations to spheroidal regions are suggested in [17, 18]. The results have also been generalized to the case with electric current sheets by Thal [19] and Hansen and Collin [20] by adding the stored energy in the interior of the sphere.

In this paper, we investigate stored electric and magnetic energy expressions based on subtraction of the far-field energy density. The expressions are suitable for antenna Q and bandwidth calculations and closely related to the classical methods in [16] and others for antenna Q calculations. They are not restricted to spherical geometries and, furthermore, resembles the recently proposed expressions by Vandenbosch [8]. The results provide a new interpretation of Vandenbosch's expressions [8] and explain the observed cases with negative stored energy [11]. They also suggest a possible remedy to the negative energy and that the computed Q has an uncertainty of the order ka, where a is the radius of the smallest circumscribing sphere and k the wavenumber. This is consistent with the use of Q for small (sub wavelength) antennas, where ka is small and Q is large [15, 16]. Analytic results for spherical structures show that the expressions in [8] for Q differ with ka from the results in [20], that is here interpreted as the far-field energy in the interior of the sphere. The results for Q are also compared with estimated values from circuit models and differentiation of the impedance [21, 22] for dipole, loop, and inverted L antennas.

The paper is organized as follows. In Sec. 2, the stored electric and magnetic energies defined be subtraction of far-field from the energy density are analyzed. Analytic results for spherical geometries and comparison with classical results are presented in Sec. 3. The coordinate dependence is analyzed in Sec. 4. Stored energies from small structures are derived in Sec. 5. Comparisons with numerical results for dipole, loop, and inverted L antennas are given in Sec. 6. The paper is concluded in Sec. 7.

2 Stored electromagnetic energy

We consider time-harmonic electric and magnetic fields, $\boldsymbol{E}(\boldsymbol{r})$ and $\boldsymbol{H}(\boldsymbol{r})$, respectively, with a suppressed $\mathrm{e}^{-\mathrm{i}\omega t}$ dependence, where ω denotes the angular

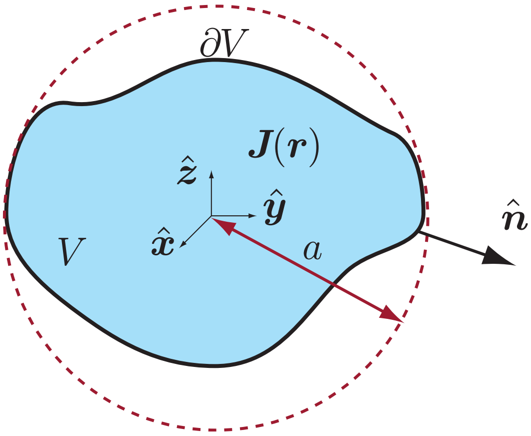

Figure 1: Illustration of the object geometry V and with outward normal unit vector $\hat{\boldsymbol{n}}$ and current density $\boldsymbol{J}(\boldsymbol{r})$. The object is circumscribed by a sphere with radius a.

frequency. The Maxwell equations in free space are [1]

$$\begin{cases} \nabla\times\boldsymbol{E} = \mathrm{i}\omega\mu_0\boldsymbol{H} = \mathrm{i}\eta_0 k\boldsymbol{H} \\ \nabla\times\boldsymbol{H} = -\mathrm{i}\omega\epsilon_0\boldsymbol{E} + \boldsymbol{J} = -\frac{\mathrm{i}k}{\eta_0}\boldsymbol{E} + \boldsymbol{J}, \end{cases} \tag{1}$$

where $\boldsymbol{J}$ denotes the current density, while ϵ_0, μ_0, and $\eta_0 = \sqrt{\mu_0/\epsilon_0}$ are the free space permittivity, permeability, and impedance, respectively. For simplicity, we interchange between the angular frequency and the free space wavenumber $k = \omega/\mathrm{c}_0$, where the speed of light $\mathrm{c}_0 = 1/\sqrt{\mu_0\epsilon_0}$. We also recall the continuity equation, $\nabla\cdot\boldsymbol{J} = \mathrm{i}\omega\rho$, relating the current density $\boldsymbol{J}$ with the charge density ρ.

It is widely accepted [1, 2, 4] that the time-harmonic electric and magnetic energy densities are $\epsilon_0|\boldsymbol{E}|^2/4$ and $\mu_0|\boldsymbol{H}|^2/4$, respectively. On the other hand, there are a few alternative suggestions in the literature [3], and the energy densities are not observable [5]. The electric and magnetic energies comprise both radiated and stored energies; however, for antenna Q calculations one must distill the stored energy. In this section we analyze stored electric and magnetic energy expressions suitable for antenna Q and bandwidth calculations, which shed new light on the meaning and practical applicability of the methodology for evaluating stored energies directly from the sources that was derived recently in [8]. In subsequent sections of this paper we elaborate the implications and practical applicability of the results of this section.

It follows from Maxwell's equations (1) that the sources and fields obey the conservation of energy equation in differential form,

$$\mathrm{i}2\omega\big(\frac{\epsilon_0}{4}|\boldsymbol{E}|^2-\frac{\mu_0}{4}|\boldsymbol{H}|^2\big)+\frac{1}{2}\boldsymbol{E}\cdot\boldsymbol{J}^*=\frac{-1}{2}\nabla\cdot(\boldsymbol{E}\times\boldsymbol{H}^*), \tag{2}$$

where the superscript * denotes complex conjugate. We consider current distributions $\boldsymbol{J}$ whose support is in a volume V bounded by the surface ∂V, see Fig. 1. Integrating (2) over this volume gives the real part result

$$\frac{\mathrm{Re}}{2}\int\limits_{\partial V}\boldsymbol{E}(\boldsymbol{r})\times\boldsymbol{H}^*(\boldsymbol{r})\cdot\hat{\boldsymbol{n}}(\boldsymbol{r})\,\mathrm{dS}=-\frac{\mathrm{Re}}{2}\int\limits_{V}\boldsymbol{E}(\boldsymbol{r})\cdot\boldsymbol{J}^*(\boldsymbol{r})\,\mathrm{dV}, \tag{3}$$

where $\hat{\boldsymbol{n}}$ denotes the outward-normal unit vector of the surface ∂V. The first term in the real part expression (3) is readily identified in view of the Poynting vector [1, 4] as the time-average radiated power flow through the surface ∂V, so that (3) equates the radiated power exiting ∂V to the time average of the power generated by $\boldsymbol{J}$, as expected from energy conservation. Furthermore, integrating (2) over all space shows that the radiated power exiting the surface ∂V can be expressed in terms of the far field as

$$P_{\mathrm{r}}=\mathrm{Re}\int\limits_{\partial V}\frac{\boldsymbol{E}(\boldsymbol{r})\times\boldsymbol{H}^*(\boldsymbol{r})\cdot\hat{\boldsymbol{n}}}{2}\,\mathrm{dS}=\int\limits_{\Omega}\frac{|\boldsymbol{F}(\hat{\boldsymbol{r}})|^2}{2\eta_0}\,\mathrm{d}\Omega, \tag{4}$$

where Ω denotes the surface of the unit sphere and the far field behaves like $\boldsymbol{E}(\boldsymbol{r})\sim\mathrm{e}^{\mathrm{i}kr}\boldsymbol{F}(\hat{\boldsymbol{r}})/r$ as $r\to\infty$, where $\boldsymbol{r}=r\hat{\boldsymbol{r}}$ and $r=|\boldsymbol{r}|$. Similarly, by integrating (2) over all space one obtains the imaginary part result

$$\int\limits_{\mathbb{R}^3}\frac{\epsilon_0}{4}|\boldsymbol{H}(\boldsymbol{r})|^2-\frac{\mu_0}{4}|\boldsymbol{E}(\boldsymbol{r})|^2\,\mathrm{dV}=\mathrm{Im}\int\limits_{V}\frac{\boldsymbol{E}(\boldsymbol{r})\cdot\boldsymbol{J}^*(\boldsymbol{r})}{4\omega}\,\mathrm{dV}, \tag{5}$$

where we used the fact that the integral of the imaginary part of the divergence term in (2) vanishes as the integration volume approaches $\mathbb{R}^3$. The imaginary part result (5) relates the well-defined difference between the time-average electric and magnetic energies with the net reactive power delivered by $\boldsymbol{J}$.

As is well known [15, 16], the total energy, defined as the integral of the energy density integrated over all space, is unbounded due to the $1/r^2$ decay of the energy density in the far radiation zone. This is resolved by decomposition of the total energy into radiated and stored energy. The stored energy is, however, difficult to define and interpret. The classical approach used by Chu [15] and Collin & Rothschild [16], and subsequently by others, is based on mode expansions, and therefore restricted to canonical geometries. Spherical regions are most commonly considered but there are also some results for cylindrical [16] and spheroidal [17, 18] structures. The stored energy density is customarily defined as the difference between the total energy density and the *radiated power flow* in the radial direction, thus the stored electric energy becomes

$$W_{\mathrm{E}}^{(\mathrm{P})} = \frac{\epsilon_0}{4} \int\limits_{\mathbb{R}^3_{\mathrm{r}}} |\boldsymbol{E}(\boldsymbol{r})|^2 - \eta_0 \,\mathrm{Re}\{\boldsymbol{E}(\boldsymbol{r}) \times \boldsymbol{H}^*(\boldsymbol{r})\} \cdot \hat{\boldsymbol{r}} \,\mathrm{dV}, \tag{6}$$

where the subscript r in $\mathbb{R}^3_{\mathrm{r}} = \{\boldsymbol{r} : \lim_{r_0\to\infty} |\boldsymbol{r}| \leq r_0\}$ is used to indicate that the integration is over an infinite spherical volume. The classical results by Chu [15] are for spheres with vanishing interior field [16], so that the stored energy is due to the exterior field only (*i.e.*, for the region where $r > a$ where a is the radius of the smallest sphere circumscribing the sources). The Thal bound [19] generalizes the results to fields generated by electric surface currents, see also [20]. Here it is observed that there is a stored energy but no radiated energy flux in the interior of the sphere. The definition (6) is useful for spherical geometries and can be generalized to cylindrical geometries [16]. It is difficult to generalize it to arbitrary geometries due to its coordinate dependence that originates from the scalar multiplication with $\hat{\boldsymbol{r}}$. The subtraction of the radiated energy flow is equivalent to subtraction of the energy of the far field outside a circumscribing sphere, *cf.*, (4). This suggests an alternative stored electric energy defined by subtraction of the *far-field energy*, *i.e.*,

$$W_{\mathrm{E}}^{(\mathrm{F})} = \frac{\epsilon_0}{4} \int\limits_{\mathbb{R}^3_{\mathrm{r}}} |\boldsymbol{E}(\boldsymbol{r})|^2 - \frac{|\boldsymbol{F}(\hat{\boldsymbol{r}})|^2}{r^2} \,\mathrm{dV}, \tag{7}$$

where the integration is over the infinite sphere $\mathbb{R}^3_{\mathrm{r}}$.

We note that the definitions with the power flow (6) and far field (7) differ only in the interior of the smallest circumscribing sphere associated with the source support. In the interior of the smallest circumscribing sphere, which we assume next to be of radius a, this subtracted far-field energy is then

$$\frac{\epsilon_0}{4} \int_0^a \int_\Omega |\boldsymbol{F}(\hat{\boldsymbol{r}})|^2 \,\mathrm{d}\Omega \,\mathrm{d}r = \frac{a}{2\mathrm{c}_0} P_{\mathrm{r}}. \tag{8}$$

Assuming that the contribution to the true stored electric energy, say W_{E}, due to the exterior field outside the smallest circumscribing sphere, is equal to that of $W_{\mathrm{E}}^{(\mathrm{P})}$ and $W_{\mathrm{E}}^{(\mathrm{F})}$ in (6) and (7), and that it subtracts some non-negative value less than $\epsilon_0|\boldsymbol{F}|^2/(4r^2)$ inside the sphere, then we obtain the bound

$$W_{\mathrm{E}}^{(\mathrm{F})} \leq W_{\mathrm{E}} \leq W_{\mathrm{E}}^{(\mathrm{F})} + \frac{a}{2\mathrm{c}_0} P_{\mathrm{r}}. \tag{9}$$

This means that the stored electric energy can be bounded from below and above by (7). The stored magnetic energy, $W_{\mathrm{M}}^{(\mathrm{F})}$, is defined analogously.

It is customary to normalize the stored energy with the radiated power to define Q-factors. The Q-factor is $Q = \max\{Q_{\mathrm{E}}, Q_{\mathrm{M}}\}$, where

$$Q_{\mathrm{E}} = \frac{2\omega W_{\mathrm{E}}}{P_{\mathrm{r}}} \quad \text{and} \quad Q_{\mathrm{M}} = \frac{2\omega W_{\mathrm{M}}}{P_{\mathrm{r}}} \tag{10}$$

and we have included a factor of 2 in the definitions of Q_{E} and Q_{M} to simplify the comparison with antenna Q. This translates the bound (9) into

$$\max\{0, Q^{(\mathrm{F})}\} \leq Q \leq Q^{(\mathrm{F})} + ka, \tag{11}$$

where we have added that Q is non-negative.

We show that the stored energy with the subtracted far field (6) is similar to the energy defined by Vandenbosch in [8] for the vacuum case. For simplicity we express the energy using the scalar potential ϕ and the vector potential $\boldsymbol{A}$ in the Lorentz gauge [1, 2, 4], so that $(\nabla^2 + k^2)\phi(\boldsymbol{r}) = -\rho(\boldsymbol{r})/\epsilon_0$ and $(\nabla^2 + k^2)\boldsymbol{A}(\boldsymbol{r}) = -\mu_0 \boldsymbol{J}(\boldsymbol{r})$ and therefore

$$\phi(\boldsymbol{r}) = \epsilon_0^{-1}(G * \rho)(\boldsymbol{r}) = \frac{1}{\epsilon_0} \int_V G(|\boldsymbol{r} - \boldsymbol{r}'|)\rho(\boldsymbol{r}')\,\mathrm{dV}' \tag{12}$$

and

$$\boldsymbol{A}(\boldsymbol{r}) = \mu_0(G * \boldsymbol{J})(\boldsymbol{r}) = \mu_0 \int_V G(|\boldsymbol{r} - \boldsymbol{r}'|)\boldsymbol{J}(\boldsymbol{r}')\,\mathrm{dV}', \tag{13}$$

where $*$ denotes convolution and G is the outgoing Green's function *i.e.*, $G(r) = \mathrm{e}^{\mathrm{i}kr}/(4\pi r)$. The vector and scalar potentials are related by $\nabla \cdot \boldsymbol{A} = \mathrm{i}k\phi/\mathrm{c}_0$ and the electric and magnetic fields are given by [1]

$$\boldsymbol{E} = \mathrm{i}\omega\boldsymbol{A} - \nabla\phi \quad \text{and} \quad \boldsymbol{H} = \mu_0^{-1}\nabla \times \boldsymbol{A}. \tag{14}$$

We also use the corresponding far-field potentials defined by

$$\phi_\infty(\hat{\boldsymbol{r}}) = \frac{1}{4\pi\epsilon_0} \int_V \rho(\boldsymbol{r}')\mathrm{e}^{-\mathrm{i}k\hat{\boldsymbol{r}}\cdot\boldsymbol{r}'}\,\mathrm{dV}' \tag{15}$$

and

$$\boldsymbol{A}_\infty(\hat{\boldsymbol{r}}) = \frac{\mu_0}{4\pi} \int_V \boldsymbol{J}(\boldsymbol{r}')\mathrm{e}^{-\mathrm{i}k\hat{\boldsymbol{r}}\cdot\boldsymbol{r}'}\,\mathrm{dV}' \tag{16}$$

giving the electric far-field

$$\boldsymbol{F}(\hat{\boldsymbol{r}}) = \mathrm{i}\omega\boldsymbol{A}_\infty(\hat{\boldsymbol{r}}) - \hat{\boldsymbol{r}}\mathrm{i}k\phi_\infty(\hat{\boldsymbol{r}}). \tag{17}$$

Using that the far-field is orthogonal to $\hat{\boldsymbol{r}}$, *i.e.*, $\hat{\boldsymbol{r}} \cdot \boldsymbol{F} = 0$, the far-field radiation pattern obeys

$$|\boldsymbol{F}|^2 = \omega^2|\boldsymbol{A}_\infty|^2 - k^2|\phi_\infty|^2. \tag{18}$$

The electric energy density is proportional to

$$
\begin{aligned}
|\boldsymbol{E}|^2 &= \omega^2|\boldsymbol{A}|^2 - 2\operatorname{Re}\{\mathrm{i}\omega\boldsymbol{A}\cdot\nabla\phi^*\} + |\nabla\phi|^2 \\
&= \omega^2|\boldsymbol{A}|^2 - 2k^2|\phi|^2 + |\nabla\phi|^2 - 2\operatorname{Re}\{\mathrm{i}\omega\nabla\cdot(\phi^*\boldsymbol{A})\},
\end{aligned} \tag{19}
$$

where we used $\nabla\cdot(\phi^*\boldsymbol{A}) = \phi^*\nabla\cdot\boldsymbol{A} + \boldsymbol{A}\cdot\nabla\phi^* = \mathrm{i}k|\phi|^2/\mathrm{c}_0 + \boldsymbol{A}\cdot\nabla\phi^*$. We integrate this result over a large sphere to get the far-field type stored electric energy (7) expressed in the potentials

$$
\begin{aligned}
\frac{4W_{\mathrm{E}}^{(\mathrm{F})}}{\epsilon_0} &= \int_{\mathbb{R}^3_{\mathrm{r}}} |\boldsymbol{E}|^2 - \frac{|\boldsymbol{F}(\hat{\boldsymbol{r}})|^2}{r^2}\,\mathrm{dV} = \int_{\mathbb{R}^3_{\mathrm{r}}} |\nabla\phi|^2 - k^2|\phi|^2 \\
&\quad + \omega^2\left(|\boldsymbol{A}|^2 - \frac{|\boldsymbol{A}_\infty|^2}{r^2}\right) - k^2\left(|\phi|^2 - \frac{|\phi_\infty|^2}{r^2}\right)\mathrm{dV},
\end{aligned} \tag{20}
$$

where we applied the divergence theorem to the integration of the last term in (19), obtaining via the discussion in (17) and (18) that $\int_\Omega \operatorname{Im}\{\phi^*(r\hat{\boldsymbol{r}})A_{\mathrm{r}}(r\hat{\boldsymbol{r}})\}r^2\,\mathrm{d}\Omega \to 0$ as $r\to\infty$, see (17).

Use the energy identity for the Helmholtz equation, $|\nabla\phi|^2 - k^2|\phi|^2 = \epsilon_0^{-1}\operatorname{Re}\{\phi\rho^*\} + \nabla\cdot(\operatorname{Re}\{\phi^*\nabla\phi\})$, and that $\phi^*\nabla\phi \to \mathrm{i}k\hat{\boldsymbol{r}}|\phi|^2$ for large enough r, to rewrite the first two terms in (20) as

$$
\begin{aligned}
\int_{\mathbb{R}^3_{\mathrm{r}}} |\nabla\phi(\boldsymbol{r})|^2 - k^2|\phi(\boldsymbol{r})|^2\,\mathrm{dV} &= \epsilon_0^{-1}\operatorname{Re}\int_V \phi(\boldsymbol{r})\rho^*(\boldsymbol{r})\,\mathrm{dV} \\
&= \int_V\int_V \rho(\boldsymbol{r}_1)\frac{\cos(k|\boldsymbol{r}_1-\boldsymbol{r}_2|)}{4\pi\epsilon_0^2|\boldsymbol{r}_1-\boldsymbol{r}_2|}\rho^*(\boldsymbol{r}_2)\,\mathrm{dV}_1\,\mathrm{dV}_2,
\end{aligned} \tag{21}
$$

where we also used that the surface term vanishes. The Green's function identity, see App. A

$$
\begin{aligned}
&\int_{\mathbb{R}^3_{\mathrm{r}}} G(|\boldsymbol{r}-\boldsymbol{r}_1|)G^*(|\boldsymbol{r}-\boldsymbol{r}_2|) - \frac{\mathrm{e}^{-\mathrm{i}k(\boldsymbol{r}_1-\boldsymbol{r}_2)\cdot\hat{\boldsymbol{r}}}}{16\pi^2r^2}\,\mathrm{dV} \\
&\qquad = -\frac{\sin(kr_{12})}{8\pi k} + \mathrm{i}\frac{r_1^2-r_2^2}{8\pi r_{12}}\,\mathrm{j}_1(kr_{12}),
\end{aligned} \tag{22}
$$

where $\mathrm{j}_1(z) = (\sin(z) - z\cos(z))/z^2$ is a spherical Bessel function [4], is used to rewrite the two remaining terms in (20) as

$$\int\limits_{\mathbb{R}^3_{\mathrm{r}}} |G * \boldsymbol{J}|^2 - \frac{|\int_V \mathrm{e}^{-\mathrm{i}k\boldsymbol{r}'\cdot\hat{\boldsymbol{r}}}\boldsymbol{J}(\boldsymbol{r}')\,\mathrm{dV}'\,|^2}{16\pi^2 r^2}\,\mathrm{dV}$$
$$= -\int\limits_V\int\limits_V \boldsymbol{J}(\boldsymbol{r}_1)\cdot\frac{\sin(k|\boldsymbol{r}_1-\boldsymbol{r}_2|)}{8\pi k}\boldsymbol{J}^*(\boldsymbol{r}_2)\,\mathrm{dV}_1\,\mathrm{dV}_2$$
$$+\,\mathrm{i}\int\limits_V\int\limits_V \boldsymbol{J}(\boldsymbol{r}_1)\cdot\frac{r_1^2-r_2^2}{8\pi r_{12}}\,\mathrm{j}_1(kr_{12})\boldsymbol{J}^*(\boldsymbol{r}_2)\,\mathrm{dV}_1\,\mathrm{dV}_2 \quad (23)$$

and

$$\int\limits_{\mathbb{R}^3_{\mathrm{r}}} |G * \rho|^2 - \frac{|\int_V \mathrm{e}^{-\mathrm{i}k\boldsymbol{r}'\cdot\hat{\boldsymbol{r}}}\rho(\boldsymbol{r}')\,\mathrm{dV}'\,|^2}{16\pi^2 r^2}\,\mathrm{dV}$$
$$= -\int\limits_V\int\limits_V \rho(\boldsymbol{r}_1)\frac{\sin(k|\boldsymbol{r}_1-\boldsymbol{r}_2|)}{8\pi k}\rho^*(\boldsymbol{r}_2)\,\mathrm{dV}_1\,\mathrm{dV}_2$$
$$+\,\mathrm{i}\int\limits_V\int\limits_V \rho(\boldsymbol{r}_1)\frac{r_1^2-r_2^2}{8\pi r_{12}}\,\mathrm{j}_1(kr_{12})\rho^*(\boldsymbol{r}_2)\,\mathrm{dV}_1\,\mathrm{dV}_2\,. \quad (24)$$

We note that the first terms in the right-hand side of (23) and (24) only depend on the distance r_{12} and are hence coordinate independent, whereas the last terms depend on the coordinate system due to the factor $r_1^2 - r_2^2 = (\boldsymbol{r}_1+\boldsymbol{r}_2)\cdot(\boldsymbol{r}_1-\boldsymbol{r}_2)$. The coordinate dependence originates in the explicit evaluation of the integral in (22) over large spherical volumes $\mathbb{R}^3_{\mathrm{r}}$ that is necessary due to the slow convergence of the integral in (22), see also App. A.

Collecting the terms in (21), (23), and (24), we get a quadratic form in the current density $\boldsymbol{J}$ for the far-field type stored electric energy (20) as

$$W_{\mathrm{E}}^{(\mathrm{F})} = W_{\mathrm{E}}^{(\mathrm{F}_0)} + W_{\mathrm{EM}}^{(\mathrm{F}_1)} + W_{\mathrm{EM}}^{(\mathrm{F}_2)}, \quad (25)$$

where $W_{\mathrm{E}}^{(\mathrm{F}_0)} + W_{\mathrm{EM}}^{(\mathrm{F}_1)}$ is the coordinate independent part

$$W_{\mathrm{E}}^{(\mathrm{F}_0)} + W_{\mathrm{EM}}^{(\mathrm{F}_1)} = \frac{\mu_0}{4}\int\limits_V\int\limits_V \nabla_1\cdot\boldsymbol{J}_1\nabla_2\cdot\boldsymbol{J}_2^*\frac{\cos(kr_{12})}{4\pi k^2 r_{12}}$$
$$-\left(k^2\boldsymbol{J}_1\cdot\boldsymbol{J}_2^* - \nabla_1\cdot\boldsymbol{J}_1\nabla_2\cdot\boldsymbol{J}_2^*\right)\frac{\sin(kr_{12})}{8\pi k}\,\mathrm{dV}_1\,\mathrm{dV}_2 \quad (26)$$

and $W_{\mathrm{E}}^{(\mathrm{F}_0)}$ and $W_{\mathrm{EM}}^{(\mathrm{F}_1)}$ contains the cos and sin parts, respectively. The coordinate dependent part is

$$W_{\mathrm{EM}}^{(\mathrm{F}_2)} = \frac{\mu_0}{4}\int_V\int_V \mathrm{Im}\left\{k^2\boldsymbol{J}_1\cdot\boldsymbol{J}_2^* - \nabla_1\cdot\boldsymbol{J}_1\nabla_2\cdot\boldsymbol{J}_2^*\right\}\frac{r_1^2-r_2^2}{8\pi r_{12}}\,\mathrm{j}_1(kr_{12})\,\mathrm{dV}_1\,\mathrm{dV}_2\,. \quad (27)$$

The coordinate independent part $W_{\mathrm{E}}^{(\mathrm{F}_0)} + W_{\mathrm{EM}}^{(\mathrm{F}_1)}$ is identical to the energy by Vandenbosch in [8] for vacuum and hence presents a clear interpretation of the energy [8] in terms of (7). We also see that the definition (7) explains the peculiar effects of negative stored energies [11] and suggests a remedy to it in (9). The coordinate dependent part $W_{\mathrm{EM}}^{(\mathrm{F}_2)}$ is more involved. Obviously the actual stored energy, as any physical quantity, should be independent of the coordinate system. First, we observe that $W_{\mathrm{EM}}^{(\mathrm{F}_2)} = 0$ for any current density that has a constant phase. This includes the fields originating from single spherical modes on spherical surfaces and hence most cases in [15, 16, 19, 20]. It also includes currents in the form of single characteristic modes [12]. We also get the coordinate independent part by taking the average of the stored energy from $\boldsymbol{J}$ and $\boldsymbol{J}^*$. The term $W_{\mathrm{EM}}^{(\mathrm{F}_2)}$ is further analyzed in Secs 4 and 5.

For the stored magnetic energy we can use $|\boldsymbol{B}|^2 = |\nabla\times\boldsymbol{A}|^2$ or simpler the energy identity (5), to directly get the difference

$$\int_{\mathbb{R}^3_{\mathrm{r}}} \mu_0|\boldsymbol{H}|^2 - \epsilon_0|\boldsymbol{E}|^2\,\mathrm{dV} = \mathrm{Re}\int_V \boldsymbol{A}\cdot\boldsymbol{J}^* - \phi\rho^*\,\mathrm{dV}, \quad (28)$$

where we used

$$\boldsymbol{E}\cdot\boldsymbol{J}^* = \mathrm{i}\omega\boldsymbol{A}\cdot\boldsymbol{J}^* - \nabla\cdot(\phi\boldsymbol{J}^*) - \mathrm{i}\omega\phi\rho^*. \quad (29)$$

This gives the far-field type stored magnetic energy $W_{\mathrm{M}}^{(\mathrm{F})} = W_{\mathrm{M}}^{(\mathrm{F}_0)} + W_{\mathrm{EM}}^{(\mathrm{F}_1)} + W_{\mathrm{EM}}^{(\mathrm{F}_2)}$, where the coordinate independent part

$$W_{\mathrm{M}}^{(\mathrm{F}_0)} + W_{\mathrm{EM}}^{(\mathrm{F}_1)} = \frac{\mu_0}{4}\int_V\int_V \boldsymbol{J}_1\cdot\boldsymbol{J}_2^*\frac{\cos(kr_{12})}{4\pi r_{12}} - \left(k^2\boldsymbol{J}_1\cdot\boldsymbol{J}_2^* - \nabla_1\cdot\boldsymbol{J}_1\nabla_2\cdot\boldsymbol{J}_2^*\right)\frac{\sin(kr_{12})}{8\pi k}\,\mathrm{dV}_1\,\mathrm{dV}_2 \quad (30)$$

is expressed as a quadratic form in $\boldsymbol{J}$, see also [8]. We also have the radiated power

$$P_{\mathrm{r}} = \frac{\eta_0}{2k}\int_V\int_V \left(k^2\boldsymbol{J}_1\cdot\boldsymbol{J}_2^* - \nabla_1\cdot\boldsymbol{J}_1\nabla_2\cdot\boldsymbol{J}_2^*\right)\frac{\sin(kr_{12})}{4\pi r_{12}}\,\mathrm{dV}_1\,\mathrm{dV}_2\,. \quad (31)$$

It is illustrative to rewrite the coordinate independent far-field stored energy in the potentials:

$$W_{\mathrm{E}}^{(\mathrm{F}_0)} = \frac{\mathrm{Re}}{4}\int_V \rho^*\phi \,\mathrm{dV}, \quad W_{\mathrm{M}}^{(\mathrm{F}_0)} = \frac{\mathrm{Re}}{4}\int_V \boldsymbol{J}^*\cdot\boldsymbol{A}\,\mathrm{dV} \tag{32}$$

and

$$W_{\mathrm{EM}}^{(\mathrm{F}_1)} = -\frac{\mathrm{Re}}{4}\int_V \frac{k}{2}\left(\boldsymbol{J}^*\cdot\frac{\partial\boldsymbol{A}}{\partial k} - \rho^*\frac{\partial\phi}{\partial k}\right)\mathrm{dV}, \tag{33}$$

where it is assumed that the frequency derivative of $\boldsymbol{J}$ and ρ are negligible in (33). We note that the sum of the first terms, $W_{\mathrm{E}}^{(\mathrm{F}_0)} + W_{\mathrm{M}}^{(\mathrm{F}_0)}$, corresponds to a frequency-domain version of the energy expression by Carpenter [5], see also [6, 7]. Moreover, they reduce to well-known electrostatic and magnetostatic expressions in the low-frequency limit [1].

It is also convenient to follow standard notation in the method of moments (MoM) and introduce the operators $\mathcal{L}_{\mathrm{e}}$ and $\mathcal{L}_{\mathrm{m}}$ such that $\mathcal{L} = \mathcal{L}_{\mathrm{e}} - \mathcal{L}_{\mathrm{m}}$ is the integral operator associated with the electric field integral equation (EFIE) [23]. Here, the operators are generalized to volumes and defined from

$$\langle\boldsymbol{J},\mathcal{L}_{\mathrm{e}}\,\boldsymbol{J}\rangle = \frac{-1}{\mathrm{i}k}\int_V\int_V \nabla_1\cdot\boldsymbol{J}(\boldsymbol{r}_1)\nabla_2\cdot\boldsymbol{J}^*(\boldsymbol{r}_2)G_{12}\,\mathrm{dV}_1\,\mathrm{dV}_2, \tag{34}$$

$$\langle\boldsymbol{J},\mathcal{L}_{\mathrm{m}}\,\boldsymbol{J}\rangle = \mathrm{i}k\int_V\int_V \boldsymbol{J}(\boldsymbol{r}_1)\cdot\boldsymbol{J}^*(\boldsymbol{r}_2)G_{12}\,\mathrm{dV}_1\,\mathrm{dV}_2, \tag{35}$$

and

$$\langle\boldsymbol{J},\mathcal{L}_{\mathrm{em}}\,\boldsymbol{J}\rangle = \frac{\mathrm{i}k}{2}\int_V\int_V \Big(\frac{1}{k}\nabla_1\cdot\boldsymbol{J}(\boldsymbol{r}_1)\nabla_2\cdot\boldsymbol{J}^*(\boldsymbol{r}_2) - k\boldsymbol{J}(\boldsymbol{r}_1)\cdot\boldsymbol{J}^*(\boldsymbol{r}_2)\Big)\frac{\partial G(k|\boldsymbol{r}_1-\boldsymbol{r}_2|)}{\partial k}\,\mathrm{dV}_1\,\mathrm{dV}_2\,. \tag{36}$$

They are defined such that the stored electric and magnetic energies and radiated power are

$$W_{\mathrm{E}}^{(\mathrm{F}_0)} = \frac{\eta_0}{4\omega}\,\mathrm{Im}\langle\boldsymbol{J},\mathcal{L}_{\mathrm{e}}\,\boldsymbol{J}\rangle \tag{37}$$

$$W_{\mathrm{M}}^{(\mathrm{F}_0)} = \frac{\eta_0}{4\omega}\,\mathrm{Im}\langle\boldsymbol{J},\mathcal{L}_{\mathrm{m}}\,\boldsymbol{J}\rangle \tag{38}$$

$$W_{\mathrm{EM}}^{(\mathrm{F}_1)} = \frac{\eta_0}{4\omega}\,\mathrm{Im}\langle\boldsymbol{J},\mathcal{L}_{\mathrm{em}}\,\boldsymbol{J}\rangle \tag{39}$$

$$P_{\mathrm{r}} = \frac{\eta_0}{2}\,\mathrm{Re}\langle\boldsymbol{J},(\mathcal{L}_{\mathrm{e}}-\mathcal{L}_{\mathrm{m}})\boldsymbol{J}\rangle. \tag{40}$$

Efficient evaluation of the $\mathcal{L}$ operator is instrumental in MoM implementations where the discretized versions are often referred to as impedance matrices. The relations above show that the corresponding matrices for the coordinate independent stored and radiated energies are available by evaluating the real and imaginary parts of the MoM impedance matrices with the addition of the mixed part (36). The stored energy is hence computed with negligible additional computational cost in MoM implementations. Moreover, (40) shows that $\operatorname{Re}\mathcal{L}$ is positive semidefinite.

3 Electric surface currents on a sphere

The two formulations (6) and (7) for the stored energy can be compared for electric surface currents on spherical shells. This is the case analyzed by Thal [19] and Hansen & Collin [20]. We expand the surface current on a sphere with radius a in vector spherical harmonics $\mathbf{Y}$, see App. B. For simplicity, consider the surface current $\boldsymbol{J}(\boldsymbol{r}) = J_0\,\mathbf{Y}_{\tau\sigma ml}(\hat{\boldsymbol{r}})\delta(r-a)$. It induces the electric and magnetic fields

$$\boldsymbol{E}(\boldsymbol{r}) = \mathrm{i}\eta_0\tilde{J}_0\frac{\mathbf{u}^{(p)}_{\tau\sigma ml}(k\boldsymbol{r})}{\mathrm{R}^{(p)}_{\tau l}(ka)} \text{ and } \boldsymbol{H}(\boldsymbol{r}) = \tilde{J}_0\frac{\mathbf{u}^{(p)}_{\bar{\tau}\sigma ml}(k\boldsymbol{r})}{\mathrm{R}^{(p)}_{\tau l}(ka)}, \tag{41}$$

where $p=1$ for $r<a$ and $p=3$ for $r>a$, $\mathbf{u}^{(p)}_{\tau\sigma ml}$ is the spherical vector waves, and $\mathrm{R}^{(p)}_{\tau l}$ the radial functions in Hansen [24], defined as

$$\mathrm{R}^{(p)}_{\tau l}(\kappa) = \begin{cases} z^{(p)}_l(\kappa) & \tau = 1 \\ \dfrac{1}{\kappa}\dfrac{\partial(\kappa z^{(p)}_l(\kappa))}{\partial\kappa} & \tau = 2, \end{cases} \tag{42}$$

where $z^{(1)}_l = \mathrm{j}_l$ are Bessel functions, $z^{(2)}_l = \mathrm{n}_l$ Neumann functions, $z^{(3)}_l = \mathrm{h}^{(1)}_l$ Hankel functions [24], and $\kappa = ka$. We note that the derivatives of $\mathrm{R}^{(p)}_{\tau l}(\kappa)$ are easily expressed in $z^{(p)}$, see App. B. Here, $\tau = 1$ is transverse electric (TE) and $\tau = 2$ transverse magnetic (TM) waves. Moreover, the dual index $\bar{\tau}$ is $\bar{\tau} = 2$ if $\tau = 1$ and $\bar{\tau} = 1$ if $\tau = 2$. The current in (41) is rescaled as $\tilde{J}_0 = J_0\,\mathrm{R}^{(1)}_{\tau l}(ka)\,\mathrm{R}^{(3)}_{\tau l}(ka)$ and below we let J_0 be real valued to simplify the notation. We also note that the coordinate dependent term (27) vanishes for single spherical modes.

3.1 Far-field type stored energy for the TE case

We start with the transverse electric (TE) case $\tau = 1$, *i.e.*, $\boldsymbol{J}(\boldsymbol{r}) = \mathbf{Y}_{1\sigma ml}(\hat{\boldsymbol{r}})\delta(r-a)$ that is divergence free, $\nabla\cdot\boldsymbol{J} = 0$. The integrals in (25) are evaluated analytical by expanding the Green's functions in (34), (35), and (36) in spherical modes, see App. B. Using $\nabla\cdot\mathbf{Y}_{1\sigma ml} = 0$, we get $\langle\boldsymbol{J},\mathcal{L}_\mathrm{e}\,\boldsymbol{J}\rangle = 0$ for (34) and hence the first part of the stored electric energy $W^{(\mathrm{F}_0)}_\mathrm{E} = 0$.

The expansion of the full Green's dyadic, $\mathbf{G} = G\mathbf{I}$, (83) gives

$$\frac{1}{\mathrm{i}k}\langle \boldsymbol{J}, \mathcal{L}_{\mathrm{m}}\, \boldsymbol{J}\rangle / J_0^2$$
$$= \int_V \int_V \mathbf{Y}_{1\sigma ml}(\hat{\boldsymbol{r}}_1)\delta(r_1 - a) \cdot \mathbf{G}_{12} \cdot \mathbf{Y}_{1\sigma ml}(\hat{\boldsymbol{r}}_2)\delta(r_2 - a)\, \mathrm{dV}_1\, \mathrm{dV}_2$$
$$= a^4 \int_\Omega \int_\Omega \mathbf{Y}_{1\sigma ml}(\hat{\boldsymbol{r}}_1) \cdot \mathbf{G}(|\boldsymbol{r}_1 - \boldsymbol{r}_2|) \cdot \mathbf{Y}_{1\sigma ml}(\hat{\boldsymbol{r}}_2)\, \mathrm{d}\Omega_1\, \mathrm{d}\Omega_2$$
$$= \mathrm{i}a^4 k\, \mathrm{R}_{1l}^{(3)}(\kappa)\, \mathrm{R}_{1l}^{(1)}(\kappa) \quad (43)$$

for the terms in (35) to get the first part of the stored magnetic energy from (38) as $4\omega\eta_0^{-1} W_{\mathrm{M}}^{(\mathrm{F}_0)} = -a^2\kappa^2 J_0^2\, \mathrm{R}_{1l}^{(2)}\, \mathrm{R}_{1l}^{(1)}$. The radiated power follow from (40) $2\eta_0^{-1} P_{\mathrm{r}} = -\operatorname{Re}\langle \boldsymbol{J}, \mathcal{L}_{\mathrm{m}}\, \boldsymbol{J}\rangle = a^2\kappa^2 J_0^2 (\mathrm{R}_{1l}^{(1)})^2$. The corresponding expansion of the frequency derivative of the Green's function (83) is used for the terms related to (36)

$$\frac{-2}{\mathrm{i}k^2 a^4}\langle \boldsymbol{J}, \mathcal{L}_{\mathrm{em}}\, \boldsymbol{J}\rangle / J_0^2$$
$$= \int_\Omega \int_\Omega \mathbf{Y}_{1\sigma ml}(\hat{\boldsymbol{r}}_1) \cdot \frac{\partial \mathbf{G}(|\boldsymbol{r}_1 - \boldsymbol{r}_2|)}{\partial k} \cdot \mathbf{Y}_{1\sigma ml}(\hat{\boldsymbol{r}}_2)\, \mathrm{d}\Omega_1\, \mathrm{d}\Omega_2$$
$$= \mathrm{i}\frac{\partial}{\partial\kappa}\Big(\kappa\, \mathrm{R}_{1l}^{(3)}(\kappa)\, \mathrm{R}_{1l}^{(1)}(\kappa)\Big) = \mathrm{i}\big(\kappa\, \mathrm{R}_{1l}^{(3)}(\kappa)\, \mathrm{R}_{1l}^{(1)}(\kappa)\big)'$$
$$= \mathrm{i}(\mathrm{R}_{1l}^{(3)}\, \mathrm{R}_{1l}^{(1)} + \kappa\, \mathrm{R}_{1l}^{(3)}{}'\, \mathrm{R}_{1l}^{(1)} + \kappa\, \mathrm{R}_{1l}^{(3)}\, \mathrm{R}_{1l}^{(1)}{}'), \quad (44)$$

where $'$ denotes differentiation with respect to κ, giving $4\omega\eta_0^{-1} W_{\mathrm{EM}}^{(\mathrm{F}_1)} = -\frac{a^2\kappa^2}{2} J_0^2 (\kappa\, \mathrm{R}_{1l}^{(2)}\, \mathrm{R}_{1l}^{(1)})'$.

Collecting the terms gives the electric and magnetic Q-factors as

$$Q_{1l,\mathrm{E}}^{(\mathrm{F})}(\kappa) = \frac{2\omega W_{\mathrm{E}}^{(\mathrm{F})}(\kappa)}{P_{\mathrm{r}}(\kappa)} = -\frac{\big(\kappa\, \mathrm{R}_{1l}^{(1)}(\kappa)\, \mathrm{R}_{1l}^{(2)}(\kappa)\big)'}{2(\mathrm{R}_{1l}^{(1)}(\kappa))^2} \quad (45)$$

and

$$Q_{1l,\mathrm{M}}^{(\mathrm{F})}(\kappa) = \frac{2\omega W_{\mathrm{M}}^{(\mathrm{F})}(\kappa)}{P_{\mathrm{r}}(\kappa)} = Q_{1l,\mathrm{E}}^{(\mathrm{F})}(\kappa) - \frac{\mathrm{R}_{1l}^{(2)}(\kappa)}{\mathrm{R}_{1l}^{(1)}(\kappa)}, \quad (46)$$

respectively. We note that $\mathrm{R}_{1l}^{(1)} = \mathrm{j}_l$ and $\mathrm{R}_{1l}^{(2)} = \mathrm{n}_l$ can be used to rewrite the Q-factors, however the form with the radial functions simplifies the comparison with the TM case below. The differentiated terms are also easily evaluated using (44) and (81).

3.2 Far-field type stored energy for the TM case

The transverse magnetic (TM) case is given by $\tau = 2$ and generated by the current density $\boldsymbol{J}(\boldsymbol{r}) = J_0 \mathbf{Y}_{2\sigma ml}(\hat{\boldsymbol{r}})\delta(r-a)$ that has the divergence $\nabla\cdot\mathbf{Y}_{2\sigma ml} = -\sqrt{l(l+1)}\,\mathrm{Y}_{\sigma ml}/r$. With the expansion of the Green's function (82) we get the part related to the charge density (34)

$$
\begin{aligned}
&-\mathrm{i}k\langle\boldsymbol{J},\mathcal{L}_{\mathrm{e}}\,\boldsymbol{J}\rangle/(a^4J_0^2)\\
&\quad=\int\limits_{\Omega}\int\limits_{\Omega}\nabla_1\cdot\mathbf{Y}_{2\sigma ml}(\hat{\boldsymbol{r}}_1)G(|\boldsymbol{r}_1-\boldsymbol{r}_2|)\nabla_2\cdot\mathbf{Y}_{2\sigma ml}(\hat{\boldsymbol{r}}_2)\,\mathrm{d}\Omega_1\,\mathrm{d}\Omega_2\\
&\quad=\frac{\mathrm{i}kl(l+1)}{a^2}\,\mathrm{j}_l(\kappa)\,\mathrm{h}_l^{(1)}(\kappa)
\end{aligned}
\tag{47}
$$

and the full Green's Dyadic expansion (83) gives

$$
\begin{aligned}
&\frac{1}{\mathrm{i}k}\langle\boldsymbol{J},\mathcal{L}_{\mathrm{m}}\,\boldsymbol{J}\rangle/(a^4J_0^2)\\
&\quad=\int\limits_{\Omega}\int\limits_{\Omega}\mathbf{Y}_{2\sigma ml}(\hat{\boldsymbol{r}}_1)\cdot\mathbf{G}(|\boldsymbol{r}_1-\boldsymbol{r}_2|)\cdot\mathbf{Y}_{2\sigma ml}(\hat{\boldsymbol{r}}_2)\,\mathrm{d}\Omega_1\,\mathrm{d}\Omega_2\\
&\quad=\mathrm{i}k\left(\mathrm{R}_{2l}^{(1)}(\kappa)\,\mathrm{R}_{2l}^{(3)}(\kappa)+l(l+1)\frac{\mathrm{h}_l^{(1)}(\kappa)\,\mathrm{j}_l(\kappa)}{\kappa^2}\right).
\end{aligned}
\tag{48}
$$

for the part related to the current density (35). The expansions of the frequency derivatives of the Green's function (82) and Green's Dyadic (83) give

$$
\begin{aligned}
&\mathrm{Re}\int\limits_{\Omega}\int\limits_{\Omega}\mathbf{Y}_{2\sigma ml}(\hat{\boldsymbol{r}}_1)\cdot\frac{\partial\mathbf{G}(|\boldsymbol{r}_1-\boldsymbol{r}_2|)}{\partial k}\cdot\mathbf{Y}_{2\sigma ml}(\hat{\boldsymbol{r}}_2)\\
&\quad-\nabla_1\cdot\mathbf{Y}_{2\sigma ml}(\hat{\boldsymbol{r}}_1)\frac{\partial\mathbf{G}(|\boldsymbol{r}_1-\boldsymbol{r}_2|)}{k^2\partial k}\nabla_2\cdot\mathbf{Y}_{2\sigma ml}(\hat{\boldsymbol{r}}_2)\,\mathrm{d}\Omega_1\,\mathrm{d}\Omega_2\\
&\quad=2l(l+1)\,\mathrm{n}_l(\kappa)\,\mathrm{j}_1(\kappa)-\kappa^2(\kappa\,\mathrm{R}_{2l}^{(1)}(\kappa)\,\mathrm{R}_{2l}^{(2)}(\kappa))'.
\end{aligned}
\tag{49}
$$

for the part related to (36).

Collecting the terms gives that the normalized radiated power is $2\eta_0^{-1}P_{\mathrm{r}}/J^2 = \mathrm{Re}\langle\boldsymbol{J},(\mathcal{L}_{\mathrm{e}}-\mathcal{L}_{\mathrm{m}})\boldsymbol{J}\rangle/J_0^2 = a^3\kappa(\mathrm{R}_{1l}^{(1)})^2$. The electric and magnetic Q factors are finally determined to

$$
Q_{2l,\mathrm{E}}^{(\mathrm{F})}(\kappa) = -\frac{\big(\kappa\,\mathrm{R}_{2l}^{(1)}(\kappa)\,\mathrm{R}_{2l}^{(2)}(\kappa)\big)'}{2(\mathrm{R}_{2l}^{(1)}(\kappa))^2}
\tag{50}
$$

and

$$
Q_{2l,\mathrm{M}}^{(\mathrm{F})} = Q_{2l,\mathrm{E}}^{(\mathrm{F})}(\kappa) - \frac{\mathrm{R}_{2l}^{(2)}(\kappa)}{\mathrm{R}_{2l}^{(1)}(\kappa)},
\tag{51}
$$

respectively. We note that the expressions for the TE case in (45) and (46) and TM case in (50) and (51) are written in identical forms by using the radial functions (42).

3.3 Power flow stored energy $W_{\mathrm{EM}}^{(\mathrm{P})}$

The stored electric energy with the subtracted power flow (6) is analyzed by Hansen & Collin [20], see also Thal [19]. The integral (6) is decomposed into integration of the exterior and interior regions where we have outgoing waves, $\mathbf{u}_{\tau\sigma ml}^{(3)}$, and regular waves, $\mathbf{u}_{\tau\sigma ml}^{(1)}$, respectively in (41). The exterior part was already analyzed by Collin & Rothschild [16]. The subtracted power flow in (6) of the fields (41) has the radial dependence

$$P_{\mathrm{r}} = \frac{\mathrm{Re}}{2}\int\limits_{\Omega} \boldsymbol{E}(\boldsymbol{r}) \times \boldsymbol{H}^{*}(\boldsymbol{r}) \cdot \hat{\boldsymbol{r}} r^2 \,\mathrm{d}\Omega = \frac{\tilde{J}_0^2 \eta_0}{2|\,\mathrm{R}_{\tau l}^{(3)}(\kappa)|^2} \tag{52}$$

in the exterior region $r \geq a$ and vanishes in the interior region $r < a$. As the spherical vector waves are orthogonal over the unit sphere they can be analyzed separately. Their integrals are divided into its angular and radial parts. To simplify the notation, we introduce the normalized energies $w_{\tau l}^{(\mathrm{e})}$ and $w_{\tau l}^{(\mathrm{i})}$ outside and inside the sphere, respectively. They are given by, see App. C for details

$$\begin{aligned} w_{1l}^{(\mathrm{e})} &= \int\limits_{\kappa}^{\infty}\int\limits_{\Omega} |\,\mathbf{u}_{1\sigma ml}^{(3)}(k\boldsymbol{r})|^2 k^2 r^2 \,\mathrm{d}\Omega - 1 \,\mathrm{d}kr \\ &= \kappa - \frac{\kappa^3}{2}\left(|\,\mathrm{h}_l^{(1)}(\kappa)|^2 - \mathrm{Re}\{\mathrm{h}_{l+1}^{(1)}(\kappa)\,\mathrm{h}_{l-1}^{(2)}(\kappa)\}\right) \end{aligned} \tag{53}$$

for $\tau = 1$ and for the $\tau = 2$ modes

$$\begin{aligned} w_{2l}^{(\mathrm{e})} &= \int\limits_{\kappa}^{\infty}\int\limits_{\Omega} |\,\mathbf{u}_{2\sigma ml}^{(3)}(k\boldsymbol{r})|^2 k^2 r^2 \,\mathrm{d}\Omega - 1 \,\mathrm{d}kr \\ &= -\,\mathrm{Re}\{\kappa\,\mathrm{h}_l^{(2)}(\kappa)(\kappa\,\mathrm{h}_l^{(1)}(\kappa))'\} + w_{1l}^{(\mathrm{e})}. \end{aligned} \tag{54}$$

The corresponding normalized energy in the interior of the sphere is given by the integrals

$$\begin{aligned} w_{1l}^{(\mathrm{i})} &= \int\limits_{0}^{\kappa}\int\limits_{\Omega} |\,\mathbf{u}_{1\sigma ml}^{(1)}(k\boldsymbol{r})|^2 k^2 r^2 \,\mathrm{d}\Omega \,\mathrm{d}kr = \int\limits_{0}^{\kappa} x^2 |\,\mathrm{j}_l(x)|^2 \,\mathrm{d}x \\ &= \frac{\kappa^3}{2}\left(\mathrm{j}_l^2(\kappa) - \mathrm{j}_{l-1}(\kappa)\,\mathrm{j}_{l+1}(\kappa)\right) \end{aligned} \tag{55}$$

and

$$w_{2l}^{(\mathrm{i})} = \int_0^{\kappa}\int_{\Omega} |\,\mathbf{u}_{2\sigma ml}^{(1)}(k\boldsymbol{r})|^2 k^2 r^2 \,\mathrm{d}\Omega\,\mathrm{d}kr$$

$$= -\operatorname{Re}\{\kappa\,\mathrm{j}_l(\kappa)(\kappa\,\mathrm{j}_l(\kappa))'\} + w_{1l}^{(\mathrm{i})}. \quad (56)$$

We have the electric and magnetic Q factors

$$Q_{\tau l,\mathrm{E}}^{(\mathrm{P})} = |\,\mathrm{R}_{\tau l}^{(3)}(\kappa)|^2 \left(\frac{w_{\tau l}^{(\mathrm{e})}(\kappa)}{|\,\mathrm{R}_{\tau l}^{(3)}(\kappa)|^2} + \frac{w_{\tau l}^{(\mathrm{i})}(\kappa)}{|\,\mathrm{R}_{\tau l}^{(1)}(\kappa)|^2}\right) \quad (57)$$

and

$$Q_{\tau l,\mathrm{M}}^{(\mathrm{P})} = |\,\mathrm{R}_{\tau l}^{(3)}(\kappa)|^2 \left(\frac{w_{\bar{\tau} l}^{(\mathrm{e})}(\kappa)}{|\,\mathrm{R}_{\tau l}^{(3)}(\kappa)|^2} + \frac{w_{\bar{\tau} l}^{(\mathrm{i})}(\kappa)}{|\,\mathrm{R}_{\tau l}^{(1)}(\kappa)|^2}\right). \quad (58)$$

After extensive simplifications we can rewrite them as

$$Q_{\tau,\mathrm{EM}}^{(\mathrm{P})}(\kappa) = \frac{2\omega W_{\mathrm{EM}}^{(\mathrm{P})}(\kappa)}{P_{\mathrm{r}}(\kappa)} = \kappa + Q_{\tau,\mathrm{EM}}^{(\mathrm{F})}(\kappa), \quad (59)$$

where $Q_{\tau,\mathrm{EM}}^{(\mathrm{F})}$ denotes the electric and magnetic far-field type Q factors in (45), (46), (50), and (51). Note that the subscript EM is used to denote E and M in (59). The difference $\kappa = ka$ is consistent with the interpretation of a standing wave in the interior of the sphere, *cf.*, (11). Moreover, the expressions (50) and (51) unifies the TE and TM cases and offer an alternative to the expressions in [20], here we also note a misprint in (6) in [20].

3.4 Numerical example for spherical shells

The electric and magnetic Q-factors are depicted in Fig. 2 for $l = 1, 2$. The relative differences are negligible for small ka where Q is large. For larger ka, where Q can be small, the relative difference is significant although the absolute difference is exactly ka. We also note that the Q factors oscillate and can be significant even for large ka. This is mainly due to small values of $\mathrm{R}_{\tau l}^{(1)}(ka)$ that can be interpreted as a negligible radiated power. Moreover, the Q-factors related to the far-field type stored energy (7) is negative in some frequency bands. The corresponding Q-factors related to (6) are always non-negative. Moreover, it is observed that $Q_{11,\mathrm{M}}^{(\mathrm{P})} \geq Q_{11,\mathrm{E}}^{(\mathrm{P})}$ for low ka but has regions with $Q_{11,\mathrm{M}}^{(\mathrm{P})} < Q_{11,\mathrm{E}}^{(\mathrm{P})}$ for larger ka.

To further analyze the negative values of (7), we depict the stored electric and magnetic energy density over spherical shells related to (7) in Fig. 3 for a TE spherical current sheet with radius $ka = 1$ and a coordinate system with origin at the center of the sphere. The results confirm that the far-field (7) and power flow (6) stored energy densities are identical outside the

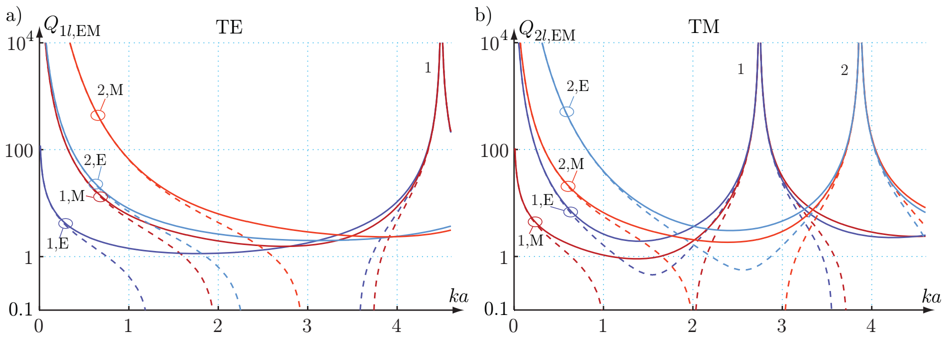

Figure 2: Electric and magnetic Q factors for electrical surface currents $\boldsymbol{J}(\boldsymbol{r}) = J_0\,\mathbf{Y}_{\tau\sigma ml}(\hat{\boldsymbol{r}})\delta(r-a)$ for $l = 1, 2$. Power (solid curves) and far-field (dashed curves) stored energies. They differ by ka (59). a) TE ($\tau = 1$) modes. b) TM ($\tau = 2$) modes.

sphere. It is also seen that the far-field stored energy density is negative in parts of the interior region of the sphere, $r < a$, whereas the power flow stored energy density is non-negative. We also notice that the stored energy density is discontinues at $r = a$ except for the far-field type stored electric energy. This is consistent with the boundary conditions that states that tangential components of the electric field are continuous.

4 Coordinate dependent term

The stored electric (25) and magnetic energies contain the potentially coordinate dependent part $W_{\text{EM}}^{(\text{F}_2)}$ defined in (27). Lets assume that $W_{\text{EM}}^{(\text{F}_2)} = W_{\text{EM},0}^{(\text{F}_2)}$ for one coordinate system. Consider a shift of the coordinate system $\boldsymbol{r} \to \boldsymbol{d} + \boldsymbol{r}$ and use that $r_1^2 - r_2^2 \to r_1^2 - r_2^2 + 2\boldsymbol{d}\cdot(\boldsymbol{r}_1 - \boldsymbol{r}_2)$. This gives the coordinate dependent term

$$W_{\text{EM},\boldsymbol{d}}^{(\text{F}_2)} = W_{\text{EM},0}^{(\text{F}_2)} + k\boldsymbol{d}\cdot\boldsymbol{W}, \tag{60}$$

where $\boldsymbol{W} = \boldsymbol{W}_\rho + \boldsymbol{W}_\text{J}$ and

$$\begin{aligned}\boldsymbol{W}_\rho &= \frac{\mathrm{i}}{2\epsilon_0}\int_V\int_V \rho_1\nabla_1\frac{\sin(kr_{12})}{8\pi k r_{12}}\rho_2^*\,\mathrm{dV}_1\,\mathrm{dV}_2\\ &= \frac{k\epsilon_0}{4}\int_\Omega \hat{\boldsymbol{r}}\Big|\int_V \frac{\rho \mathrm{e}^{-\mathrm{i}k\hat{\boldsymbol{r}}\cdot\boldsymbol{r}}}{4\pi\epsilon_0}\,\mathrm{dV}\Big|^2\,\mathrm{d}\Omega = \frac{k\epsilon_0}{4}\int_\Omega |\phi_\infty|^2\hat{\boldsymbol{r}}\,\mathrm{d}\Omega\end{aligned} \tag{61}$$

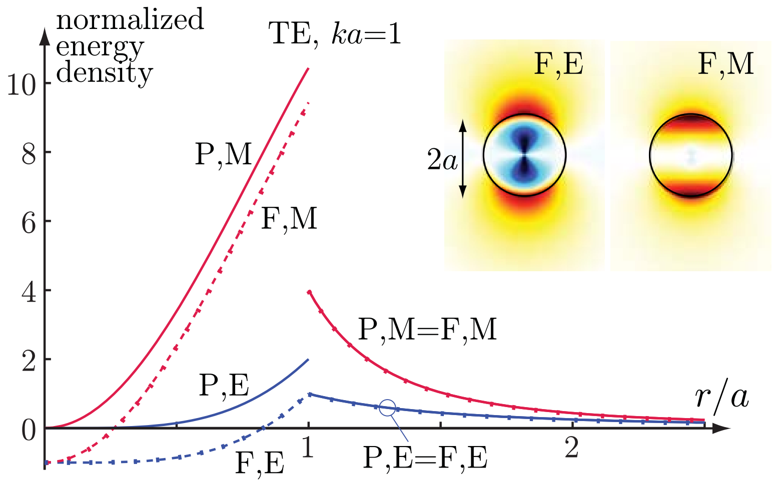

Figure 3: Illustration of the stored electric (E) and magnetic (M) energy densities for the TE ($\tau = 1$) mode generated by currents on a spherical shell with radius $ka = 1$. Power (solid curves-P) and far-field (dashed curves-F) stored energies. The energy densities are normalized with the radiated power and integrated over spherical shells to emphasize the radial dependence. The angular distribution is also depicted.

and we used (77), the identity

$$\nabla_1 \frac{\sin(kr_{12})}{4\pi kr_{12}} = -\mathrm{i}k \lim_{r\to\infty} \int\limits_{|\boldsymbol{r}|=r} \hat{\boldsymbol{r}} G_1 G_2^* \,\mathrm{dS} = -\frac{\mathrm{i}k}{16\pi^2} \lim_{r\to\infty} \int\limits_{\Omega} \hat{\boldsymbol{r}} \mathrm{e}^{-\mathrm{i}k\hat{\boldsymbol{r}}\cdot(\boldsymbol{r}_1-\boldsymbol{r}_2)} \,\mathrm{d}\Omega, \quad (62)$$

and the far-field potential (15). Similarly, the current part is

$$\boldsymbol{W}_{\mathrm{J}} = -\frac{\mathrm{i}\mu_0}{2} \int\limits_V \int\limits_V \boldsymbol{J}_1 \cdot \boldsymbol{J}_2^* \nabla_1 \frac{\sin(kr_{12})}{8\pi kr_{12}} \,\mathrm{dV}_1 \,\mathrm{dV}_2 = -\frac{1}{4\mu_0} k \int\limits_{\Omega} |\boldsymbol{A}_\infty|^2 \hat{\boldsymbol{r}} \,\mathrm{d}\Omega. \quad (63)$$

And with (18) totally

$$\boldsymbol{W} = -\frac{\epsilon_0}{4k} \int\limits_{\Omega} |\boldsymbol{F}(\hat{\boldsymbol{r}})|^2 \hat{\boldsymbol{r}} \,\mathrm{d}\Omega. \quad (64)$$

The corresponding Q factor is shifted as

$$\varDelta Q_{\mathrm{EM}}^{(\mathrm{F}_2)} = \frac{-k\boldsymbol{d}\cdot\int_{\Omega}\hat{\boldsymbol{r}}|\boldsymbol{F}(\hat{\boldsymbol{r}})|^2\,\mathrm{d}\Omega}{2\int_{\Omega}|\boldsymbol{F}(\hat{\boldsymbol{r}})|^2\,\mathrm{d}\Omega}, \tag{65}$$

where we see that $|\varDelta Q_{\mathrm{EM}}^{(\mathrm{F}_2)}| \leq ka$ for all coordinate shifts within the smallest circumscribing sphere.

Consider a spherical current sheet to illustrate the coordinate dependence. Let the far field be $\boldsymbol{F} \sim \alpha_1\,\mathrm{Y}_{1\mathrm{e}01} + \alpha_2\,\mathrm{Y}_{2\mathrm{o}11}$, *i.e.*, a combination of a $\hat{\boldsymbol{z}}$ directed magnetic dipole and a $\hat{\boldsymbol{y}}$ directed electric dipole. This gives $\varDelta Q_{\mathrm{EM}}^{(\mathrm{F}_2)} = -kx/4$ and with a coordinate system centered in the sphere also $Q_{\mathrm{EM},\boldsymbol{0}}^{(\mathrm{F}_2)} = 0$ as then $r_1 = r_2$ giving $Q_{\mathrm{EM},\boldsymbol{d}}^{(\mathrm{F}_2)} = -kx/4$, where $x = \boldsymbol{d}\cdot\hat{\boldsymbol{x}}$ and $\boldsymbol{d}$ is the vector to the center of the sphere.

5 Small structures

Evaluation of the stored energy for antenna Q is most interesting for small structures, where Q is large, *e.g.*, $Q \geq 10$, and can be used to quantify the bandwidth of antennas [10, 11, 15, 21, 22]. The low-frequency expansion of the stored energy are presented in [8–11]. Here, we base it on the low-frequency expansion $\boldsymbol{J} = \boldsymbol{J}^{(0)} + k\boldsymbol{J}^{(1)} + \mathcal{O}(k^2)$ as $k \to 0$, where $\nabla\cdot\boldsymbol{J}^{(0)} = 0$ and the static terms $\boldsymbol{J}^{(0)}$ and $\rho_0 = -\mathrm{i}\nabla\cdot\boldsymbol{J}^{(1)}/\mathrm{c}_0$ have a constant phase.

It is illustrative to compare the corresponding asymptotic expansions of the Q-factor components in (25). The coordinate dependent part vanishes if $\boldsymbol{J}$ and $\rho(\boldsymbol{r})$ have constant phase. This gives

$$\begin{aligned}
&\mathrm{Im}\{\rho(\boldsymbol{r}_1)\rho^*(\boldsymbol{r}_2)\}\\
&\qquad= \mathrm{Im}\{(\rho_0(\boldsymbol{r}_1) + k\rho_1(\boldsymbol{r}_1))(\rho_0^*(\boldsymbol{r}_2) + k\rho_1^*(\boldsymbol{r}_2))\} + \mathcal{O}(k^2)\\
&\qquad\qquad= k\,\mathrm{Im}\{\rho_0(\boldsymbol{r}_1)\rho_1^*(\boldsymbol{r}_2) + \rho_1(\boldsymbol{r}_1)\rho_0^*(\boldsymbol{r}_2)\} + \mathcal{O}(k^2)
\end{aligned} \tag{66}$$

as $k \to 0$ and similarly for $\boldsymbol{J}$. The different parts of the stored energy (25) contribute to the Q-factor asymptotically

$$Q_{\mathrm{EM}}^{(\mathrm{F}_0)} \sim \frac{1}{(ka)^3},\ Q_{\mathrm{EM}}^{(\mathrm{F}_1)} \sim \frac{1}{ka},\ Q_{\mathrm{EM}}^{(\mathrm{F}_2)} \sim ka \tag{67}$$

as $ka \to 0$, where a is the radius of smallest circumscribing sphere and the coordinate system is centered inside the sphere.

We can compare the expansion (67) with the Chu bound [15]

$$Q_{\mathrm{Chu}} = \frac{1}{(ka)^3} + \frac{1}{ka}, \tag{68}$$

where it is seen that Q_{Chu} has components that are of the same order as $Q_{\mathrm{EM}}^{(\mathrm{F}_0)}$ and $Q_{\mathrm{EM}}^{(\mathrm{F}_1)}$ and hence that these terms are essential to produce reliable results. This is also the conclusion from Sec. 3 in (59), where it is shown that the Q-factors differ by ka.

The coordinate dependent part $Q_{\mathrm{EM}}^{(\mathrm{F}_2)}$ is negligible for small structures and of the same order as the difference between the far-field (7) and power (6) type as seen by the bound (11). We also note that the importance of Q diminishes as Q approaches unity. This also restricts the interest of the results to small antennas. The importance of $Q_{\mathrm{EM}}^{(\mathrm{F}_2)}$ for larger structures can however not be neglected.

6 Antenna examples

6.1 Strip dipole

Consider a center fed strip dipole with length ℓ and width $\ell/100$ modeled as perfectly electric conducting (PEC). The Q-factors (10) determined from the integral expressions $Q_{\mathrm{E}}^{(\mathrm{F})}$ in (26) and $Q_{\mathrm{M}}^{(\mathrm{F})}$ in (30), the circuit model [25], and differentiation of the impedance [21, 22] are compared in 4a. The circuit model is based on a the circuit representations of the lowest order spherical modes [26] with the lumped elements determined with the approach in [25]. The Q-factors from the circuit model approximates the integral expression very well for $\ell < 0.3\lambda$ but starts to differ for shorter wavelengths where the circuit model is less accurate. The Q factors from the *differentiated impedance* is [21, 22]

$$Q^{(\mathrm{Z})}(\omega_0) = \frac{\omega_0 |Z'_{\mathrm{m}}|_{\omega=\omega_0}}{2R(\omega_0)}, \tag{69}$$

where $'$ denotes differentiation with respect to ω and Z_{m} is the impedance $Z = R + \mathrm{j}X$, with $\mathrm{j} = -\mathrm{i}$, tuned to resonance with a lumped series (or analogous for lumped elements in parallel) inductor or capacitor

$$Z_{\mathrm{m}}(\omega) = Z(\omega) - \begin{cases} \mathrm{j}X(\omega_0)\omega/\omega_0 & \text{if } X(\omega_0) < 0 \\ \mathrm{j}X(\omega_0)\omega_0/\omega & \text{if } X(\omega_0) > 0. \end{cases} \tag{70}$$

In addition to the Q factor in (69), we determine the stored energy in the lumped element normalized with the radiated power as

$$\varDelta Q^{(\mathrm{Z})}(\omega_0) = \frac{|X(\omega_0)|}{R(\omega_0)} \tag{71}$$

giving the electric and magnetic Q factors

$$Q_{\mathrm{E}}^{(\mathrm{Z})} = \begin{cases} Q^{(\mathrm{Z})} & \text{if } X(\omega_0) < 0 \\ Q^{(\mathrm{Z})} - \varDelta Q^{(\mathrm{Z})} & \text{if } X(\omega_0) > 0 \end{cases} \tag{72}$$

and

$$Q_{\mathrm{M}}^{(\mathrm{Z})} = \begin{cases} Q^{(\mathrm{Z})} & \text{if } X(\omega_0) > 0 \\ Q^{(\mathrm{Z})} - \varDelta Q^{(\mathrm{Z})} & \text{if } X(\omega_0) < 0, \end{cases} \tag{73}$$

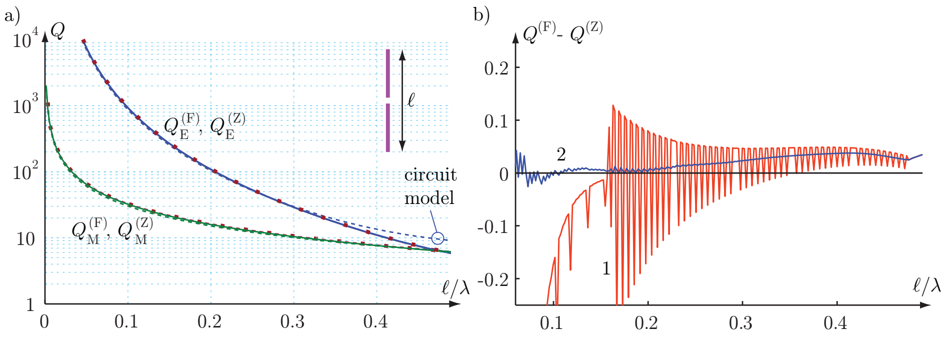

Figure 4: Illustration of the Q factor for a center feed strip dipole with length ℓ and width $\ell/100$. The Q factors are determined from the stored energies (26) and (30) and from differentiation of the impedance (72) and (73). a) electric and magnetic Q-factors from (26), (30), the circuit model (dashed curves), and differentiation of the impedance $Q^{(\mathrm{Z})}$. b) difference between the computed Q-factors $Q^{(\mathrm{F})} - Q^{(\mathrm{Z})}$, where $Q^{(\mathrm{Z})}$ is computed from a difference scheme and analytic differentiation of a high order rational approximation in 1 and 2, respectively.

respectively.

The difference $Q^{(\mathrm{F})} - Q^{(\mathrm{Z})}$ is also depicted in 4b. It is seen that the difference is negligible for the considered wavelengths. Curve (1) shows $Q^{(\mathrm{Z})}$ computed with a finite difference scheme. The curve is sensitive to noise and the used discretization. The noise is suppressed by approximating the impedance with a high order polynomial and performing analytic differentiation as seen by curve (2).

6.2 Loop antenna

The computed stored electric and magnetic energies for a loop antenna are depicted in Fig. 5. The loop antenna is rectangular with height ℓ, width $\ell/2$, vanishing thickness, and is modeled as perfectly electric conducting (PEC). It is seen that the magnetic energy dominates for low frequencies. It changes to dominantly electric energy at approximately $\lambda \approx 6\ell$ or equivalently $\lambda \approx C/2$, where $C = 3\ell$ denotes the circumference of the loop.

In Fig. 5, it is seen that the Q-factors determined from the stored energies (26) and (30) and from differentiation of the impedance agree very well for $Q \geq 10$. The difference increases for lower Q values. This is consistent with the increasing difficulties to approximate the impedance with a single resonance model [22] and the potential ka ambiguity of the far-field stored energy (11). Here, it is also important to realize that the concept and usefulness of the Q-factor is increasingly questionable as Q decreases towards unity.

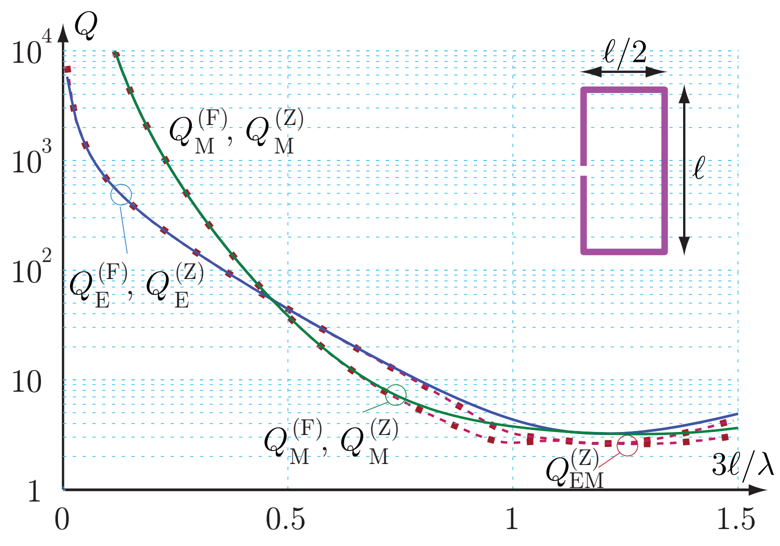

Figure 5: Illustration of the Q factor for a rectangular loop antenna with height ℓ and width $\ell/2$. The Q factors are determined from the stored energies (26) and (30) and from differentiation of the impedance (72) and (73).

6.3 Inverted L antenna

An inverted L antenna on a finite ground plane is considered to illustrate the usefulness of the stored energies for terminal antennas. The antenna has total length ℓ and width $\ell/2$, see Fig. 6. The electric and magnetic Q factors are depicted in Fig. 6. It is seen that $Q_{EM}^{(F)}$ and $Q_{EM}^{(Z)}$ agree well for $Q \geq 10$, that is for approximately $\ell \geq \lambda/3$ or below 1 GHz for 10 cm chassis. The results start to differ for larger structures, where *e.g.*, $Q_E^{(F)} \approx 5$ and $Q_E^{(Z)} \approx 2$ at $\ell/\lambda = 0.4$ or $ka \approx 1.4$. For this levels of $Q^{(Z)}$, the underlying single resonance model [22] is problematic and hence $Q^{(Z)}$ reduce in accuracy. Moreover, $Q_E^{(F)}$ as an approximation of Q have a relatively large uncertainty bound (11) for $ka \approx 1.4$. At the same time Q is low enough to be considered less useful as a quantity to estimate the bandwidth, *e.g.*, $Q \approx 2$ corresponds to a half-power bandwidth of 100%.

7 Conclusions

The analyzed expression (7) for the stored energy defined by subtraction of the far-field energy density from the energy density is mainly motivated by the formulation of Collin & Rothschild [16] and the expressions by Vandenbosch in [8]. We show that the stored energy (7) is identical to the energy in [8] for many currents. However, some current densities have an additional

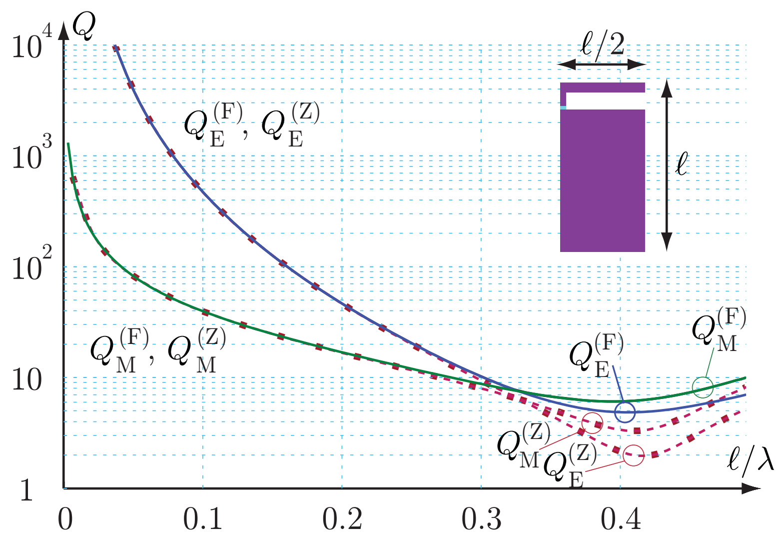

Figure 6: Illustration of the Q factor for an inverted L antenna. The circumscribing rectangle has height ℓ and width $\ell/100$. The Q factors are determined from the stored energies (26) and (30) and from differentiation of the impedance (72) and (73).

coordinate dependent term. This term is very small for small antennas but it can contribute for larger structures. Here, it is also important to realize that the classical definition [16] with the subtracted power flow (6) is inherently coordinate dependent. The identification of the energy expressions in [8] with (7) offers simple interpretation of the observed cases with a negative stored energy [11]. The analysis also suggests that the resulting Q factor has an uncertainty of the order ka. This is consistent with the use of the results for small (sub wavelength) antennas [11, 13], where ka is small and Q large.

The energy expressions proposed by Vandenbosch in [8] are very well suited for optimization formulations as they are simple quadratic forms of the current density. The quadratic form is very practical as it allows for various optimization formulations such as Lagrangian [11] and convex optimization [13] and has already led to many new antenna results. Their resemblance of the electric field integral equation (EFIE) makes the numerical implementation very simple. Analytic solutions for spherical structures show that the Q in [8] and [20] differ by ka and this is interpreted as the far-field in the interior of the sphere as seen from (7) and (6). The new formulation also produce simplified expressions (59) the unifies the TE and TM cases for the Q factor of current densities on spherical shells [20]. Numerical results for dipole, loop, and inverted L antennas are also used to illustrate the accuracy of the energy expressions.

8 Acknowledgments

This work was supported by the Swedish Research Council (VR), the Crafoord Foundation, and the Swedish Governmental Agency for Innovation Systems (VINNOVA) within the VINN Excellence Center CHASE. Prof. Edwin Marengo at Northeastern University, MA, USA is also acknowledged for valuable discussions and his hospitably during a visit of MG to Boston in August 2012.

A Green's function identities

Multiply the Helmholtz Green's function for G_1: $(\nabla^2 + k^2)G_1 = -\delta(\boldsymbol{r} - \boldsymbol{r}_1)$ with G_2^*, and similarly for G_2^*. Adding the results together with a standard vector calculus identity gives $2(\nabla G_1 \cdot \nabla G_2^* - k^2 G_1 G_2^*) = G_1\delta_2 + G_2^*\delta_1 + \nabla^2(G_1 G_2^*)$. Integration yields the identity [8]

$$\int\limits_{\mathbb{R}^3_{\mathrm{r}}} \nabla G(|\boldsymbol{r} - \boldsymbol{r}_1|) \cdot \nabla G^*(|\boldsymbol{r} - \boldsymbol{r}_2|) - k^2 G(|\boldsymbol{r} - \boldsymbol{r}_1|)G^*(|\boldsymbol{r} - \boldsymbol{r}_2|)\,\mathrm{dV} = \frac{\cos(k|\boldsymbol{r}_1 - \boldsymbol{r}_2|)}{4\pi|\boldsymbol{r}_1 - \boldsymbol{r}_2|}, \quad (74)$$

where we used Gauss's theorem together with the observation that $\nabla(G_1 G_2^*) \to -\hat{\boldsymbol{r}}\mathrm{e}^{\mathrm{i}k\hat{\boldsymbol{r}}\cdot(\boldsymbol{r}_2 - \boldsymbol{r}_1)}/(8\pi^2 r^3)$ for large enough radius.

The k-derivative of the Helmholtz Green's equation for G_1 is $(\nabla^2 + k^2)\partial_k G_1 + 2kG_1 = 0$. Similarly to the derivation of (74) we multiply with G_2^*, and repeat the procedure with the k-derivative of G_2^*. Adding the result and applying vector calculus identities to move ∇^2 away from the k-derivative results in the identity

$$4kG_1G_2^* = \delta_2\partial_k G_1 + \delta_1\partial_k G_2^* - \nabla\cdot\boldsymbol{q}, \quad (75)$$

where

$$\begin{aligned}\hat{\boldsymbol{r}}\cdot\boldsymbol{q} = \hat{\boldsymbol{r}}\cdot(G_1\nabla\partial_k G_2 - (\partial_k G_2^*)\nabla G_1 + G_2^*\nabla\partial_k G_1 \\ - (\partial_k G_1)\nabla G_2^*) \to \frac{-k}{8\pi^2 r}\Big[2 + \frac{1}{r}\big(\hat{\boldsymbol{r}}\cdot(\boldsymbol{r}_1 + \boldsymbol{r}_2) \\ + \mathrm{i}[|\hat{\boldsymbol{r}}\times\boldsymbol{r}_1|^2 - |\hat{\boldsymbol{r}}\times\boldsymbol{r}_2|^2]\big) + \mathcal{O}(\frac{1}{r^2})\Big]\mathrm{e}^{-\mathrm{i}k\hat{\boldsymbol{r}}\cdot(\boldsymbol{r}_1 - \boldsymbol{r}_2)} \quad (76)\end{aligned}$$

for large enough radius. Collecting term of decay rate r^{-1} on the left-hand side and the remaining terms on the right-hand side. Integration over a large sphere, together with Gauss's theorem and elementary integrals results in

$$\begin{aligned}
\int\limits_{\mathbb{R}^3_{\mathrm{r}}} G(|\boldsymbol{r}-\boldsymbol{r}_1|)G^*(|\boldsymbol{r}-\boldsymbol{r}_2|) - \frac{\mathrm{e}^{-\mathrm{i}k(\boldsymbol{r}_1-\boldsymbol{r}_2)\cdot\hat{\boldsymbol{r}}}}{16\pi^2 r^2}\,\mathrm{dV} \\
= -\frac{\sin(kr_{12})}{8\pi k} + \mathrm{i}\frac{r_1^2-r_2^2}{8\pi k^2 r_{12}^3}(\sin(kr_{12}) - kr_{12}\cos(kr_{12})) \\
= -\frac{\sin(kr_{12})}{8\pi k} + \mathrm{i}\frac{(\boldsymbol{r}_1+\boldsymbol{r}_2)\cdot(\boldsymbol{r}_1-\boldsymbol{r}_2)}{8\pi r_{12}}\,\mathrm{j}_1(kr_{12}) \\
= -\frac{\sin(kr_{12})}{8\pi k} - \mathrm{i}\frac{(\boldsymbol{r}_1+\boldsymbol{r}_2)}{k}\cdot\nabla_1\frac{\sin(kr_{12})}{8\pi k r_{12}}.
\end{aligned} \tag{77}$$

Here $\mathrm{j}_1(z) = (\sin(z) - z\cos(z))/z^2$ and $r_{12} = |\boldsymbol{r}_1 - \boldsymbol{r}_2|$. Note that (77) generalizes the result in [8] to the case $\boldsymbol{r}_1 + \boldsymbol{r}_2 \neq \mathbf{0}$ and shows that the integral depends of the coordinate system. It also shows that it is necessary to specify how the integration over $\mathbb{R}^3$ is performed, *i.e.*, here as the limit $\mathbb{R}^3_{\mathrm{r}} = \{\boldsymbol{r} : \lim_{r_0\to\infty} |\boldsymbol{r}| < r_0\}$.

B Spherical waves

The radiated electromagnetic field is expanded in spherical vector waves or modes [24]:

$$\begin{cases}
\mathbf{u}^{(p)}_{1\sigma ml}(k\boldsymbol{r}) = \mathrm{R}^{(p)}_{1l}(kr)\,\mathbf{Y}_{1\sigma ml}(\hat{\boldsymbol{r}}) \\
\mathbf{u}^{(p)}_{2\sigma ml}(k\boldsymbol{r}) = \mathrm{R}^{(p)}_{21}(kr)\,\mathbf{Y}_{2\sigma ml}(\hat{\boldsymbol{r}}) + \widetilde{\mathrm{R}}(kr)\,\mathrm{Y}_{\sigma ml}(\hat{\boldsymbol{r}})\hat{\boldsymbol{r}} \\
\mathbf{u}^{(p)}_{3\sigma ml}(k\boldsymbol{r}) = z^{(p)\prime}_{l}(kr)\,\mathrm{Y}_{\sigma ml}(\hat{\boldsymbol{r}})\hat{\boldsymbol{r}} + \widetilde{\mathrm{R}}(kr)\,\mathbf{Y}_{2\sigma ml}(\hat{\boldsymbol{r}})
\end{cases} \tag{78}$$

where $\boldsymbol{r}$ is the spatial coordinate, $\hat{\boldsymbol{r}} = \boldsymbol{r}/r$, $r = |\boldsymbol{r}|$, k the wavenumber, $\widetilde{\mathrm{R}}(\kappa) = \sqrt{l(l+1)}z^{(p)}_l(\kappa)/\kappa$, and $\mathrm{R}^{(p)}_l(kr)$ are the radial function of order l:

$$\mathrm{R}^{(p)}_{\tau l}(\kappa) = \begin{cases} z^{(p)}_l(\kappa) & \tau = 1 \\ \dfrac{1}{\kappa}\dfrac{\partial(\kappa z^{(p)}_l(\kappa))}{\partial\kappa} & \tau = 2. \end{cases} \tag{79}$$

For regular waves ($p = 1$) $z^{(1)}_l = \mathrm{j}_l$ is a spherical Bessel function, irregular waves ($p = 2$) $z^{(2)}_l = \mathrm{n}_l$ is a spherical Neumann function, and outgoing waves ($p = 3$) $z^{(3)}_l = \mathrm{h}^{(1)}_l$ is an outgoing spherical Hankel function. The indices are $l = 1, \dots,$ $m = 0, \dots, l$, $\sigma = \{\mathrm{e}, \mathrm{o}\}$, see [27, 28]. In addition, $\mathbf{Y}_{\tau\sigma ml}(\hat{\boldsymbol{r}})$ denotes the vector spherical harmonics defined as

$$\mathbf{Y}_{1\sigma ml}(\hat{\boldsymbol{r}}) = \frac{1}{\sqrt{l(l+1)}}\nabla\times\big(\boldsymbol{r}\,\mathrm{Y}_{\sigma ml}(\hat{\boldsymbol{r}})\big) \tag{80}$$

and $\mathbf{Y}_{2\sigma ml}(\hat{\boldsymbol{r}}) = \hat{\boldsymbol{r}} \times \mathbf{Y}_{1\sigma ml}(\hat{\boldsymbol{r}})$ where $\mathrm{Y}_{\sigma ml}$ denotes the ordinary spherical harmonics [28]. There are a few alternative definitions of the spherical vector waves in the literature [24, 27, 28]. Here, we follow [27] and use $\cos m\phi$ and $\sin m\phi$ as basis functions in the azimuthal coordinate. This choice is motivated by the interpretation of the fields related to the first 6 modes as the fields from different Hertzian dipoles. The modes labeled by $\tau = 1$ (odd ν) are TE modes (or magnetic 2^l-poles) while those labeled by $\tau = 2$ (even ν) correspond to TM modes (or electric 2^l-poles). We note that the derivatives of $\mathrm{R}_{\tau n}^{(p)}(\kappa)$ are easily expressed in spherical Bessel and Hankel functions, *i.e.*,

$$\frac{\partial\,\mathrm{R}_{\tau l}^{(p)}}{\partial\kappa} = \begin{cases} \dfrac{\partial}{\partial\kappa} z_l^{(p)} & \tau = 1 \\ \dfrac{-\,\mathrm{R}_{\tau l}^{(p)}}{\kappa} + \dfrac{l(l+1)-\kappa^2}{\kappa^2} z_l^{(p)} & \tau = 2. \end{cases} \tag{81}$$

The Green functions are expanded in spherical waves to analyze spherical geometries. The scalar Green's function has the expansion [28]

$$\begin{aligned} G(\boldsymbol{r}_1 - \boldsymbol{r}_2) = {} & \frac{\mathrm{e}^{\mathrm{i}k|\boldsymbol{r}_1-\boldsymbol{r}_2|}}{4\pi|\boldsymbol{r}_1-\boldsymbol{r}_2|} \\ & = \mathrm{i}k \sum_{\sigma ml} \mathrm{j}_l(kr_<)\,\mathrm{h}_l^{(1)}(kr_>)\,\mathrm{Y}_{\sigma ml}(\hat{\boldsymbol{r}}_1)\,\mathrm{Y}_{\sigma ml}(\hat{\boldsymbol{r}}_2), \end{aligned} \tag{82}$$

where $r_< = \min\{|\boldsymbol{r}_1|, |\boldsymbol{r}_2|\}$ and $r_> = \max\{|\boldsymbol{r}_1|, |\boldsymbol{r}_2|\}$, and $\mathrm{Y}_{\sigma ml}$ denotes the spherical harmonics. In addition, the full Green's dyadic, $\mathbf{G} = \mathbf{I}G$, can be expanded as [28]

$$\mathbf{G}(\boldsymbol{r}_1 - \boldsymbol{r}_2) = \mathrm{i}k \sum_{\tau\sigma ml} \mathbf{u}_{\tau\sigma ml}^{(1)}(k\boldsymbol{r}_<)\,\mathbf{u}_{\tau\sigma ml}^{(3)}(k\boldsymbol{r}_>), \tag{83}$$

where $\tau = 1, 2, 3$. We also use the frequency derivatives of the Green's function and the Green's dyadic expansions.

C Volume integrals

The volume integrals of the spherical vector waves are given by integrals of spherical Hankel functions as evaluated here. We have

$$\int x^2 z_p^2(x)\,\mathrm{d}x = \frac{x^3}{2}\left(z_p^2(x) - z_{p-1}(x) z_{p+1}(x)\right). \tag{84}$$

For the spherical Hankel function $z_p = \mathrm{h}_p^{(1)} = \mathrm{j}_p + \mathrm{i}\,\mathrm{n}_p$ we have

$$\int x^2 |\,\mathrm{h}_p^{(1)}(x)|^2\,\mathrm{d}x = \frac{x^3}{2}\left(|\,\mathrm{h}_p^{(1)}(x)|^2 - \mathrm{Re}\{\mathrm{h}_{p-1}^{(1)}(x)\,\mathrm{h}_{p+1}^{(1)*}(x)\}\right). \tag{85}$$

To evaluate the stored reactive energy outside a sphere, we need the result

$$\int_a^{\infty} \left(x^2 |\, \mathrm{h}_p^{(1)}(x)|^2 - 1\right) \mathrm{d}x$$
$$= a - \frac{a^3}{2}\left(|\, \mathrm{h}_p^{(1)}(a)|^2 - \mathrm{Re}\{\mathrm{h}_{p-1}^{(1)}(a)\, \mathrm{h}_{p+1}^{(1)*}(a)\}\right). \quad (86)$$

The corresponding internal energy is

$$\int_0^a x^2 |\, \mathrm{j}_p^{(2)}(x)|^2 \,\mathrm{d}x = \frac{a^3}{2}\left(\mathrm{j}_p^2(a) - \mathrm{j}_{p-1}(a)\, \mathrm{j}_{p+1}(a)\right). \quad (87)$$

We also have for $\tau = 1$

$$\int_{[a,b]\times\Omega} |\, \mathbf{u}_{1\sigma ml}(k\boldsymbol{r})|^2 \,\mathrm{dV} = \int_a^b |\, \mathrm{h}_l^{(1)}(kr)|^2 r^2 \,\mathrm{d}r \quad (88)$$

For $\tau = 2$, we use

$$\begin{aligned} k|\, \mathbf{u}_{2\sigma ml}\,|^2 = k\, \mathbf{u}_{2\sigma ml} \cdot \mathbf{u}_{2\sigma ml}^* &= \nabla \times \mathbf{u}_{1\sigma ml} \cdot \mathbf{u}_{2\sigma ml}^* \\ &= \nabla \cdot (\mathbf{u}_{1\sigma ml} \times \mathbf{u}_{2\sigma ml}^*) + \mathbf{u}_{1\sigma ml} \cdot \nabla \times \mathbf{u}_{2\sigma ml}^* \\ &= \nabla \cdot (\mathbf{u}_{1\sigma ml} \times \mathbf{u}_{2\sigma ml}^*) + k|\, \mathbf{u}_{1\sigma ml}\,|^2 \end{aligned} \quad (89)$$

and hence

$$\int_{[a,b]\times\Omega} |\, \mathbf{u}_{2\sigma ml}(k\boldsymbol{r})|^2 \,\mathrm{dV} = \frac{1}{k}\,\mathrm{Re}\left[\mathrm{h}_l^{(1)*}\, \frac{\mathrm{R}_{2l}^{(3)}}{kr} r^2\right]_a^b + \int_a^b |\, \mathrm{h}_l^{(1)}(kr)|^2 r^2 \,\mathrm{d}r, \quad (90)$$

where we have used the Wronskian relation $z^* z' - z'^* z = -2\mathrm{i}/x^2$, for $z = \mathrm{h}_l^{(1)}(x)$, and the recursion relations for the spherical Hankel functions [4] in the last steps. The terms can be evaluated as $b \to \infty$ by considering the asymptotic behavior of the spherical Hankel functions.

References

[1] J. D. Jackson, *Classical Electrodynamics*, 3rd ed. New York: John Wiley & Sons, 1999.

[2] L. D. Landau, E. M. Lifshitz, and L. P. Pitaevskiĭ, *Electrodynamics of Continuous Media*, 2nd ed. Oxford: Pergamon, 1984.

[3] R. P. Feynman, R. B. Leighton, and M. Sands, *The Feynman Lectures on Physics*. Reading, MA, USA: Addison-Wesley, 1965.

[4] J. van Bladel, *Electromagnetic Fields*, 2nd ed. Piscataway, NJ: IEEE Press, 2007.

[5] C. Carpenter, "Electromagnetic energy and power in terms of charges and potentials instead of fields," *IEE Proc. A*, vol. 136, no. 2, pp. 55–65, 1989.

[6] V. Endean and C. Carpenter, "Electromagnetic energy and power in terms of charges and potentials instead of fields (comments with reply)," in *IEE Proc. A*, vol. 139, no. 6. IET, 1992, pp. 338–342.

[7] M. Uehara, J. Allen, and C. Carpenter, "Electromagnetic energy and power in terms of charges and potentials instead of fields (comments with reply)," in *IEE Proc. A*, vol. 139, no. 1. IET, 1992, pp. 42–44.

[8] G. A. E. Vandenbosch, "Reactive energies, impedance, and Q factor of radiating structures," *IEEE Trans. Antennas Propagat.*, vol. 58, no. 4, pp. 1112–1127, 2010.

[9] W. Geyi, "Physical limitations of antenna," *IEEE Trans. Antennas Propagat.*, vol. 51, no. 8, pp. 2116–2123, Aug. 2003.

[10] G. A. E. Vandenbosch, "Simple procedure to derive lower bounds for radiation Q of electrically small devices of arbitrary topology," *IEEE Trans. Antennas Propagat.*, vol. 59, no. 6, pp. 2217–2225, 2011.

[11] M. Gustafsson, M. Cismasu, and B. L. G. Jonsson, "Physical bounds and optimal currents on antennas," *IEEE Trans. Antennas Propagat.*, vol. 60, no. 6, pp. 2672–2681, 2012.

[12] M. Capek, P. Hazdra, and J. Eichler, "A method for the evaluation of radiation Q based on modal approach," *IEEE Trans. Antennas Propagat.*, vol. 60, no. 10, pp. 4556–4567, 2012.

[13] M. Gustafsson and S. Nordebo, "Antenna currents for optimal Q, superdirectivity, and radiation patterns using convex optimization," *IEEE Trans. Antennas Propagat.*, 2012, (in press).

[14] P. Hazdra, M. Capek, and J. Eichler, "Radiation Q-factors of thin-wire dipole arrangements," *Antennas and Wireless Propagation Letters, IEEE*, vol. 10, pp. 556–560, 2011.

[15] L. J. Chu, "Physical limitations of omni-directional antennas," *J. Appl. Phys.*, vol. 19, pp. 1163–1175, 1948.

[16] R. E. Collin and S. Rothschild, "Evaluation of antenna Q," *IEEE Trans. Antennas Propagat.*, vol. 12, pp. 23–27, Jan. 1964.

[17] H. Foltz and J. McLean, "Limits on the radiation Q of electrically small antennas restricted to oblong bounding regions," in *IEEE Antennas and Propagation Society International Symposium*, vol. 4. IEEE, 1999, pp. 2702–2705.

[18] J. C.-E. Sten, P. K. Koivisto, and A. Hujanen, "Limitations for the radiation Q of a small antenna enclosed in a spheroidal volume: axial polarisation," *AEÜ Int. J. Electron. Commun.*, vol. 55, no. 3, pp. 198–204, 2001.

[19] H. L. Thal, "New radiation Q limits for spherical wire antennas," *IEEE Trans. Antennas Propagat.*, vol. 54, no. 10, pp. 2757–2763, Oct. 2006.

[20] R. Hansen and R. Collin, "A new Chu formula for Q," *IEEE Antennas and Propagation Magazine*, vol. 51, no. 5, pp. 38–41, 2009.

[21] A. D. Yaghjian and S. R. Best, "Impedance, bandwidth, and Q of antennas," *IEEE Trans. Antennas Propagat.*, vol. 53, no. 4, pp. 1298–1324, 2005.

[22] M. Gustafsson and S. Nordebo, "Bandwidth, Q-factor, and resonance models of antennas," *Progress in Electromagnetics Research*, vol. 62, pp. 1–20, 2006.

[23] J. Jin, *Theory and computation of electromagnetic fields.* Wiley Online Library, 2010.

[24] J. E. Hansen, Ed., *Spherical Near-Field Antenna Measurements*, ser. IEE electromagnetic waves series. Stevenage, UK: Peter Peregrinus Ltd., 1988, no. 26, ISBN: 0-86341-110-X.

[25] M. Gustafsson, "Sum rules for lossless antennas," *IET Microwaves, Antennas & Propagation*, vol. 4, no. 4, pp. 501–511, 2010.

[26] H. L. Thal, "Exact circuit analysis of spherical waves," *IEEE Trans. Antennas Propagat.*, vol. 26, no. 2, pp. 282–287, Mar. 1978.

[27] R. F. Harrington, *Time Harmonic Electromagnetic Fields.* New York: McGraw-Hill, 1961.

[28] A. Boström, G. Kristensson, and S. Ström, "Transformation properties of plane, spherical and cylindrical scalar and vector wave functions," in *Field Representations and Introduction to Scattering*, ser. Acoustic, Electromagnetic and Elastic Wave Scattering, V. V. Varadan, A. Lakhtakia, and V. K. Varadan, Eds. Amsterdam: Elsevier Science Publishers, 1991, ch. 4, pp. 165–210.